PS/Int. EA 60 - 10
12th September 1960

PROPOSAL FOR AN EXPERIMENT TO DETECT NEUTRINO INDUCED REACTIONS

SUMMARY

We have studied the possibility of detecting neutrino induced reactions at CERN, by means of heavy liquid bubble chambers. In estimating the expected rates we have assumed the validity of calculations based on the conventional Fermi theory. The rate of "simple" collisions (as differentiated from collisions in which additional pions are produced) is expected to be of the order of one event per day per ton of sensitive detecting material, in agreement with an estimate made by Bernardini[1]. The shielding requirements and several alternative physical arrangements have been studied. It is concluded that proper arrangement of 4,000 tons of heavy concrete and 650 tons of steel should reduce the potentially confusing background to a negligible level.

1. INTRODUCTION

It has recently been pointed out that a study of neutrino induced reactions at high energy should contribute incisively to the understanding of the weak interactions[2,3]. We present here

1) G. Bernardini, Rochester, Conference on High Energy Nuclear Physics (1960).

2) B. Pontecorvo, J. Exptl. Theoret. Phys. (U.S.S.R.) 37, 1751 (1959)
M. Schwartz, Phys. Rev. Letters 4, 306 (1960).

3) T.D. Lee and C.N. Yang, Phys. Rev. Letters 4, 307 (1960)
Y. Yamaguchi, Prog. Theo. Phys. 23, 1117 (1960)
N. Cabbibo and R. Gatto, Nuovo Cimento 15, 304 (1960)

a study of the feasibility of initiating experiments in this direction at CERN. The experiment considered here uses as neutrino source the pions produced in an internal target at the PS. The neutrinos are separated from all other particles by means of a thick shield in front of the detector. We consider here in detail the questions of : 1) How to obtain the highest neutrino flux. 2) How much shielding is necessary and 3) What is the expected detection rate.

The latter involves necessarily the use of a theoretical cross section estimate. For this we have used the prediction of the conventional Fermi theory. The rates which have been computed[3] on this basis are those for the "simple" processes :

$$\left.\begin{array}{l} \nu + n \longrightarrow e^- + p \\ \qquad\longrightarrow \mu^- + p \end{array}\right\} \quad \text{I}$$

$$\left.\begin{array}{l} \bar{\nu} + p \longrightarrow e^+ + n \\ \qquad\longrightarrow \mu^+ + n \end{array}\right\} \quad \text{II}$$

The theoretical cross sections for these reactions are represented by $\sigma(\nu)$, in Fig. 1. Besides these, reactions in which pions are produced in addition, such as $\nu + n \longrightarrow e^- + p + \pi^o$, etc., are expected to proceed with comparable cross sections, but no detailed calculations on these "complex" rates are available at present.

These reactions are characterized by the emission of leptons of several hundred Mev/c momentum (see appendix A1 for the kinematics). In the bubble chamber one will see then a minimum ionizing particle originating in the chamber, perhaps surrounded by a nuclear star. It is expected that the background of similar events due to other particles than neutrinos will be reduced to an insignificant level by shielding. All such events will therefore be ascribable to neutrinos. In addition, electrons and positrons will almost always be identifiable as such by their characteristic radiation (change

in momentum) and its reconversion into pairs. In some fraction of the cases (perhaps 1/3) of muon production, the muon will stop in the chamber and can be identified.

2. NEUTRINO BEAM

2.1 Question of internal vs external target

The external proton beam at the PS is expected to be ready in about one year. Are the advantages of the external beam such that the experiment should be delayed until that time ? We believe not, even if one should succeed in ejecting the entire internal beam. In general an internal target is struck more efficiently than an external target. It is thin, and by multiple traversal all protons are expected to react. The secondaries are not reabsorbed. The unavoidable targeting loss due to the diffraction scattering of the protons out of their orbit, should not be more than about 30 %. On the other hand, the optimum target thickness in the external beam is 1 nuclear mean free path, and this represents a targeting loss, in part due to reactions of the secondaries, of $1 - \frac{1}{e}$ or 63 %. On the other hand, with the internal target it is necessary to use mesons produced at about 6^{o} or more. This reduces the effective flux by about a factor 1.5 with respect to an external target, where the forward π's can be used. The two factors combine to give a slight advantage to the internal target. We should mention here that it may be possible to do better with an external target by the use of a long, thin, low density target to avoid secondary interactions of the emitted mesons, and a focusing channel of the sort used by Citron for the SC muon beam. This suggestion, for which we are indebted to M.G.M.Hine, has not yet been studied in detail, but is not expected to yield an improvement

sufficient to change the conclusion that there is no compelling reason to wait for the external beam.

2.2 Details of the pion (neutrino) fluxes associated with internal targets

This problem is essentially that of the behaviour of the pion trajectories in the fringing field of the following magnet sections. Detailed calculations have been made of the bending as well as focussing effects for several target positions. These are presented in appendix A2.

It can be seen from these results, as is also immediatly understandable, that the behaviours of positive and negative mesons are quite different. Now the theoretical cross sections for antineutrinos (produced by negative π's) are three to four times smaller than those for neutrinos (positive π's) in the most important energy region at the PS (Fig. 1). We have therefore tried to optimise the π^+ flux, with an attending sacrifice of the π^- flux. The π^+ beam is characterized by horizontal defocusing and vertical focusing. The vertical increase in intensity more than compensates the horizontal decrease (see Fig. 7, 8, 9 and 11 in A2), the detector and the angle with respect to the internal proton beam can be taken to maximise the flux at the energy which is expected to contribute most strongly to neutrino events. This condition can be easily satisfied with a target in section 5 and the chamber in the normal bubble chamber area.

3. SHIELDING

The shielding must reduce the intensity of strongly interacting particles above 500 Mev, which produce confusing reactions especially neutrons to less than say one confusing reaction in 100 days. In

addition, other background should be reduced to a level which will make scanning of the pictures easy. We have made some preliminary background measurements with the small chamber of Hahn. On the basis of these measurements and simple calculations (see appendix A3) we arrive at the following shielding requirements: 15 m of heavy concrete between the machine and the chamber, three meters around the sides and back of the chamber, as well as 50 cm of iron as roof. In addition about 4 m of iron in the line of sight should be sufficient to reduce the μ background to several per picture. A few μ's per picture are desirable to monitor the operation of the chamber.

The roof of iron, together with the shielding inherent in the magnet of the chamber, should also be adequate against cosmic rays.

4. LAYOUTS

Two possible layouts for the experiment are shown in Fig. 2. They are essentially equivalent from the point of view of expected reaction rates, as will be shown later. Of the two, the one which keeps the bubble chamber in the area reserved for it (layout 1) requires somewhat more concrete shielding. This small disadvantage is more than compensated by the advantage of being able to prepare the experiment without interfering with others.

In all, 650 tons of iron and 4,000 tons of heavy concrete shielding will be required for layout 1.

5. RATE OF NEUTRINO EVENTS/DAY

The expected rate of neutrino events per day is :

$$R = \eta_1 \eta_2 \eta_3 I_p Q N \frac{W}{2} \frac{1}{L^2} \sum_i \int \sigma^i_{eff}(p) \left(1 - e^{-\delta/\lambda p}\right) A^i(p) \frac{\partial^2 N}{\partial p \partial \omega} dp$$

where η_1 is the efficiency of the detector, e.g. fraction of chamber volume useful for analysis

η_2 is the target efficiency

η_3 is proportion of the useful machine time

I_p is number of circulating protons per pulse of the machine

Q is theoretical number of machine pulses per day

N is Avogadro's number

W is total mass of the detector sensitive volume

L is distance target-detector

$\sigma^i_{eff}(p)$ is the effective neutrino cross-section for process i (Fig.1) and pions of momentum p. The expression for $\sigma_{eff}(p)$ will be immediately clear if it is remembered that the neutrino spectrum from π decay is flat and extends from about zero to 0.425 of the pion momentum for high energy pions.

$$\sigma^i_{eff}(p) = \frac{1}{0.425\ p} \int_0^{0.425\ p} \sigma^i(\nu)\ dp_\nu$$

where p is the momentum of the decaying pion and p_ν is the momentum of the neutrino. $\sigma_{eff}(p)$ is plotted in Fig. 1.

$1 - \exp(-s/\lambda p)$ is the decay probability for pion decay, s is the distance target-shielding wall, λ is the decay constant (55 m $\text{Gev}^{-1}c$)

$A^i(p)$ is the amplification of solid angle subtended by the detector, due to the fringing field (Fig.11, A2). It is discussed in A2.

$\partial^2 N/\partial p \partial \omega$ is the lab spectrum for pion production by 25 Bev protons

The following parameters are used

$$\eta_1 \eta_2 \eta_3 = \frac{1}{3}$$

$$I_p = 3 \times 10^{11}$$

$$Q = 29{,}000$$

$$W = 0.75 \times 10^6 \text{ g.}$$

$\frac{\partial^2 N}{\partial p \partial \omega}$ is taken from the statistical calculations of v.Behr and Hagedorn[4] which have been verified experimentally to some extend.

The expected rates of "simple" neutrino events per day are given in Table 1.

The considerations above are virtually independent of the type of detector. What counts is the total sensitive mass of detector to obtain a desired rate of neutrino events.

---

4) J. v.Behr and R. Hagedorn, CERN Report 60-20.

TABLE 1

Expected rates of "simple" neutrino events per day for three layouts studied in this report.

Target in straight section	5	2	1
Layout	1(Fig.2)	2(Fig.2)	2(Fig.2)
Target-detector L (m)	75	49	56
Decay Path s (m)	43	27	34
Detector angle	7.2^{o}	5.7^{o}	7.2^{o}
Amplification of solid angle	Fig.11a	Fig.11b	Fig.11c
"Simple" neutrino events per day	0.55	0.62	0.54

6. ACKNOWLEDGEMENTS

It is a pleasure to acknowledge interesting discussions with Drs. G. Bernardini, G. Cocconi, H. Faissner, B. Hyams, W. Love and C.A. Ramm, the generous help of Dr. B. Hahn who not only put his freon chamber at the disposal of this study, but personally conducted the operation, as well as the kind assistance of Drs. F. Bullock, G.E. Kalmus, B. Kuiper, G. Plass and the Computor group.

7. CONCLUSION

We find then that it should be feasible to detect neutrino induced reactions in heavy liquid chambers at the PS, and that the rate which one might expect is of the order of 1 event per day per ton of sensitive detecting material. As already stated, this figure is virtually independent of the type of detector; so that in view of the considerable effort to be put into the project, any other suitable detector should run in parallel with the bubble chamber. A run of 2 to 3 weeks would be sufficient to settle the question, repeatedly raised, of whether or not there are two types of neutrinos (if there are two kinds, no reactions involving electrons or positrons will be observed). The shielding requirements, although formidable, seem manageable. We therefore propose that such an exposure should be actively prepared.

In particular, the arrangement of layout 1 seems favourable since it gives roughly maximum rate of event, and at the same time:

a) it requires no dislocation of the bubble chamber;

b) it interferes little or not at all with other experiments. In principle, simultaneous running with some other experiments is not excluded.

c) It leaves the possibility of using the external proton beam, when it becomes available, since the proton beam points roughly in that direction.

/sl (pool)

F. Krienen
R.A. Salmeron
J. Steinberger

Distribution : (open)
PBC group
Parameter Committee

APPENDICES

A1. KINEMATICS

Figures 3, 4, 5 and 6 summarize the Kinematics of reactions

$$\nu + n \longrightarrow p + e^- \qquad (1)$$

$$\nu + n \longrightarrow p + \mu^- \qquad (2)$$

The full lines are curves of constant neutrino energy. The dotted lines, in all diagrams, are curves of constant angle of emission of the proton in the center of mass system. Figures 3 and 5 show the angle of emission of the proton as a function of the proton momentum in the lab. system. Figures 4 and 6 show the similar relation for the electrons of reaction (1) and muons of reaction (2) respectively.

A2. PARTICLE OPTICS

In order to compute the rate of neutrino events per day, a study of the influence of the stray field of the machine on the pion flux was made. We used the computer programme of Kuiper, Lake and Plass[5], which calculates the trajectories of a particle of given charge and momentum in the median plane of the magnetic field of the accelerator. This programme prints out the apparent angle of emission y' and the apparent target position y with respect to a coordinate system fixed at the starting point (e.g. the target) of the trajectory. These two quantities are useful to plot the trajectory in the Experimental Hall. Figures 7, 8 and 9 show a

---

5) B. Kuiper, D. Lake and G. Plass, Report PS/Int.EA 59-14.

plot of y and y' against the real angle of emission from the target, y'_o , with the momentum as parameter. Those diagrams are related to the various target positions considered in this report, i.e. the target in pump manifold of straight section 1, 2 and 5 respectively. The radial position of the target is fixed to what seems, for the time being, the most reliable position of operation, i.e. on the equilibrium orbit.

The focusing in the median plane may be found exactly by plotting in the graph the points corresponding to the sides of the detector. If w is the width of the detector and $\Delta y'_o$ the angular interval of emission corresponding to this width, then the amplification in the median plane is given by $A_H = L \Delta y'_o / w$. If w is small enough, so that the corresponding intervals on the y and on the y' curves are essentially straight it may be shown that A_H takes the form

$$A_H = \left| \frac{1}{\frac{dy'}{dy'_o} + \frac{dy}{dy'_o} / L} \right|$$

In Fig. 10a is shown the typical case of the bending of positive particles. Under the above conditions they seem to emerge from a fixed (image) point. Consequently an equivalent lens system can be set up, Fig. 10b, and the location and the strength of the lens is found from the relations :

$$v + b = - dy/dy'$$

$$v/b = - dy'/dy'_o$$

$$1/v + 1/b = 1/f$$

leading to the formula for the amplification A_H in the median plane. As there is not yet a computer programme to calculate the trajectory outside the median plane, the focusing in the vertical plane has to be evaluated by plotting the field gradients along an actual track, requiring thus a large amount of work. If however the

particle stays no longer than, say, one magnet section in the strayfield, thin lens approximation seems to give reliable results. The equivalent lens system is obtained by changing the sign of the lens as computed for the case of the median plane and keeping the same location. This is shown in Fig. 10c leading to a similar expression for the amplification A_V in the vertical plane.

The product $A(p) = A_H \cdot A_V$ gives the overall amplification of solid angle subtended by the detector, for a particle of momentum p. In the case of thin lens approximation this expression is simple, containing elements which can be read from the median plane graphs (Figs. 7, 8 and 9) :

$$A(p) = \left| \frac{1}{\left\{ \frac{dy'}{dy'_o} + \frac{dy}{dy'_o}/L \right\} \left\{ 2 - \frac{dy'}{dy'_o} - \frac{dy}{dy'_o}/L \right\}} \right|$$

According to this equation the magnification is larger than unity if

$$1 - \sqrt{2} < \frac{dy'}{dy'_o} + \frac{dy}{dy'_o}/L < 1 + \sqrt{2}$$

From the detector location that we have chosen it follows that this condition is met for all positive particles and the higher energy negative particles. The amplification factor A(p) is plotted in Fig. 11. For this computation thin lens approximation was used for the negative particles, but for the positive particles A_V was obtained by integrating numerically the trajectory in the magnetic field.

Remark about the region of $y'_o < 0$ of Figs. 7, 8 and 9

These diagrams are based on computations made by varying y'_o in steps of 10 milliradians. The bumps observed in the region of $y'_o < 0$ might then hide some more abrupt variations of some of the curves which could only be noticed with smaller intervals of y'_o.

A3. BACKGROUND

The problem to reduce the unwanted interactions to a level where neutrino events may be clearly distinguishable is probably dependent on the choice of the detector. The background comes from muons and strong interacting particles from the machine and from cosmic rays. In the case of a bubble chamber the shielding against muons should be on the basis of, say, 5 muon tracks per picture, so as to ease the scanning. The shielding against muons is mainly through the ionization loss of the muons, which for heavy concrete is about 2 MeV $cm^2\ g^{-1}$. A shielding wall of 7,000 $g\ cm^{-2}$, i.e. 20 m of heavy concrete, will cut off the muon spectrum below 14 GeV. If $\partial^2 N/\partial p \partial \omega$ is the differential pion production spectrum, the number of muons penetrating the shielding is, with some minor simplifications :

$$C_\mu = n \frac{1}{L^2} \int_{Pmin}^{Pmax} \frac{\partial^2 N}{\partial p \partial \omega} f_1(p)\, f_2(p)\, dp \quad \text{muons } m^{-2} \text{ pulse}^{-1}$$

in which n is the number of interacting protons per pulse,

$1/L^2$ is the solid angle subtended by 1 m^2 at L meter from the target,

p is the pion momentum,

p_{max} is the maximum pion momentum produced in the direction of the detector,

p_{min} is the cut off muon momentum as a consequence of a given shielding thickness,

$f_1(p)$ is the fraction of the solid angle in the rest system of the decaying pion which contains muons with momentum in the lab above p_{min}.

$$f_1(p) \approx 2.35 \frac{p-p_{min}}{p}$$

$f_2(p)$ is the pion decay probability

$$f_2(p) \approx \frac{s}{55p}$$

On the basis of Hagedorn's lab spectra[4], the muon flux has been calculated for a number of p_{min} and of angles θ of pion emission from target. The results are given in table 2. $\partial^2 N/\partial p \partial \omega$ has been multiplied by a factor 2/3 to account for the charged pions only. In each case L and s have been adapted to the shielding thickness according to

$$L = 2s = 3p_{min} + 8,$$

with L and s in meters and p_{min} in GeV/c.

From table 2 may be seen that for low muon flux in the detector the shielding wall should have a corresponding momentum cut off nearly equal to the maximum pion momentum at given angle.

A shielding wall satisfying the condition for low muon flux has a thickness of 9000 g cm^{-2} or more and is necessary only in the direction of line of sight. The shield in front of the chamber, but not in direct line of sight need not be as heavy. It should reduce the intensity of neutrons of energy above 0.5 Bev (which can produce confusing reactions in the chamber) to less than about 10^{-6} per m^2 per pulse. If the absorption mean free path in the heavy concrete shielding is 140 g/cm^2, then 5200 g/cm^2 or 15 m of heavy concrete should be sufficient in the forward directions.

TABLE 2

Number of muons m^{-2}. $pulse^{-1}$ as a function of the cutt off muon momentum, p_{min}, and angle of emission of pions from the target, θ.

$$\frac{2}{3} n \frac{1}{L^2} \int_{p_{min}}^{p_{max}} \frac{\partial^2 N}{\partial p \partial \omega} \times 2.35 \frac{p-p_{min}}{p} \times \frac{s}{55p} \, dp$$

($n = 3 \times 10^{11}$; $L = 2s = 3\, p_{min} + 8$, p_{min} in GeV/c)

p_{min} \ θ	1^o	3^o	5^o	10^o
10	7.0×10^5	6.8×10^5	4.3×10^5	3.5×10^4
12	1.8×10^5	1.5×10^5	8.6×10^4	4.2×10^3
14	3.5×10^4	2.6×10^4	1.5×10^4	2.2×10^2
16	1.1×10^4	5.8×10^3	3.1×10^3	4.5
18	1.9×10^3	1.1×10^3	3.9×10^2	0
20	2.4×10^2	1.0×10^2	2.7×10^1	0
22	1.6×10^1	4.5	0	0

The cosmic rays flux of neutrons above 500 MeV is of the order of 1 m^{-2} $ster^{-1}$ s^{-1}. Discrimination against the age of the tracks in the chamber would reduce this rate by a factor of 1000. So above the chamber about 7 absorption lengths are required to reduce the counting rate in the detector to 10^{-6} neutrons m^{-2} $pulse^{-1}$. The chamber body, the coils and the magnet steel account for about 4 absorption lengths, so a roof of at least 400 g cm^{-2} has to be added. It is recommended to extend this roof over the whole area of the block house and to make the roof of solid steel. In this case the roof is self-supported and allows the crane to pass overhead, facilitating considerably the problem of erection and repair on the chamber.

SIS. R/1916

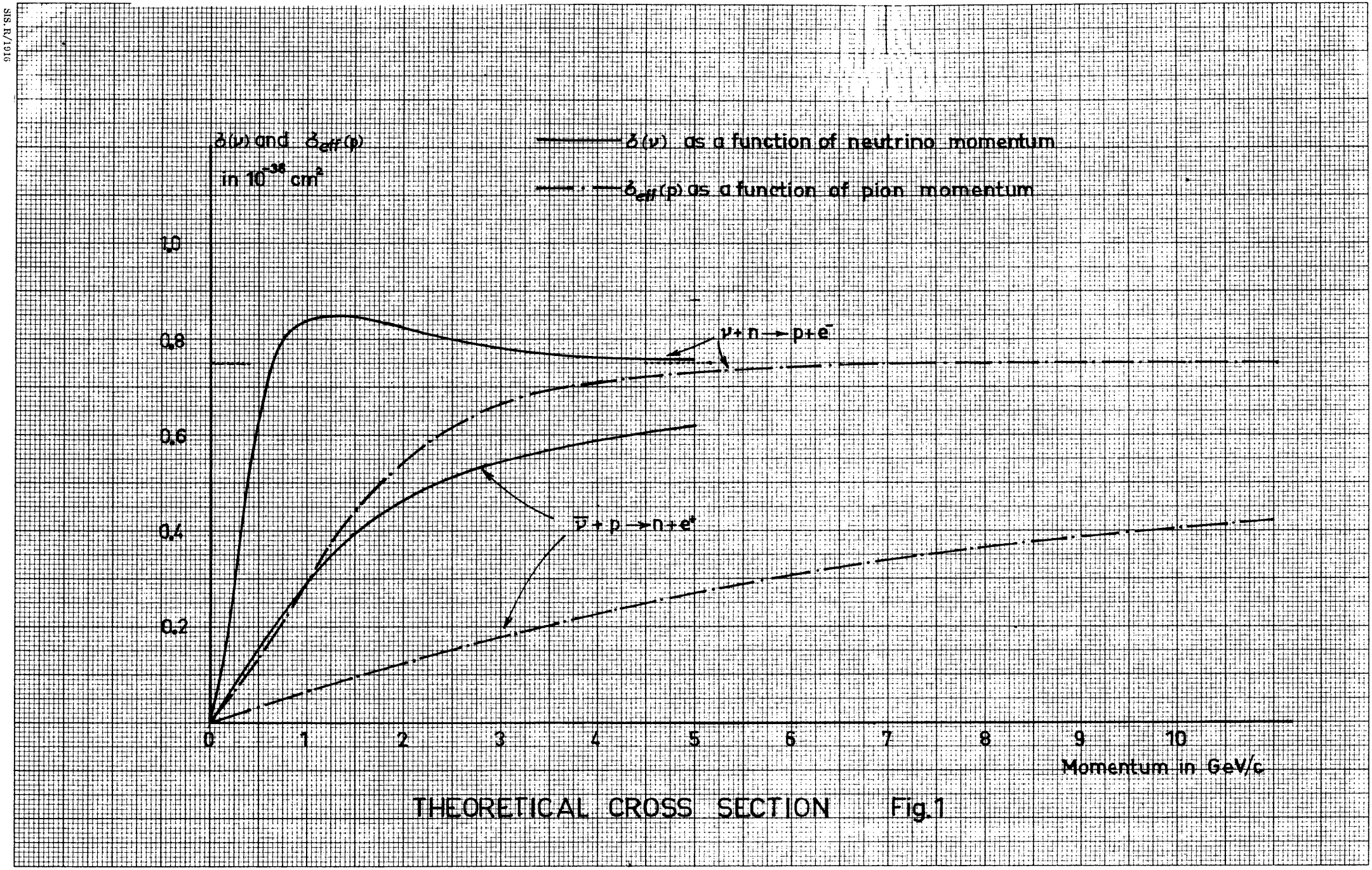

THEORETICAL CROSS SECTION Fig.1

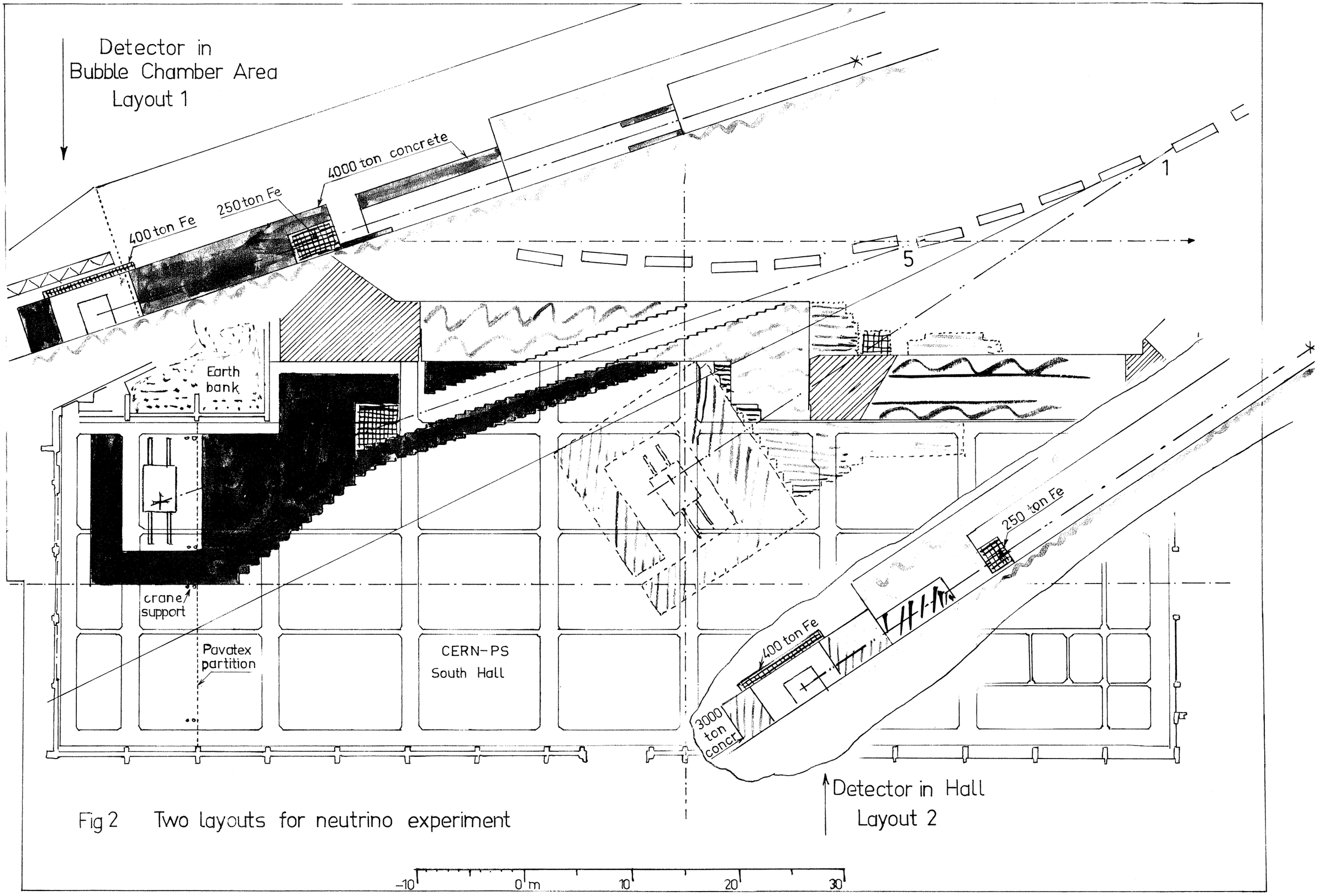

Fig 2 Two layouts for neutrino experiment

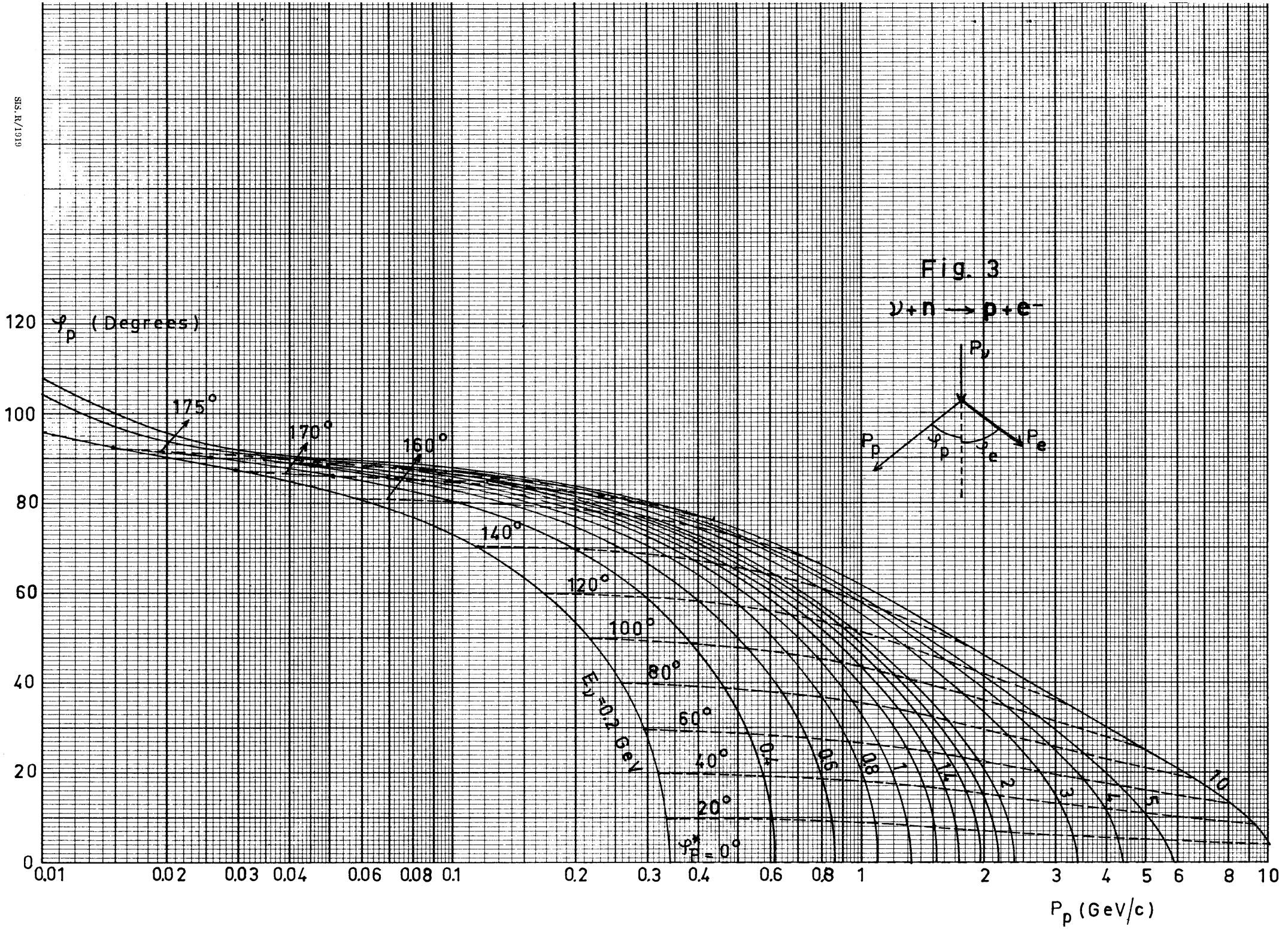
Fig. 3
ν + n → p + e⁻
φ_p (Degrees)
P_p (GeV/c)
P_ν
P_p
P_e
φ_p
φ_e
175°
170°
160°
140°
120°
100°
80°
60°
40°
20°
$\varphi_p^* = 0°$
E_ν = 0.2 GeV
0.4
0.5
0.8
1
1.4
2
3
4
5
10
0
20
40
60
80
100
120
0.01
0.02
0.03
0.04
0.06
0.08
0.1
0.2
0.3
0.4
0.6
0.8
1
2
3
4
5
6
8
10

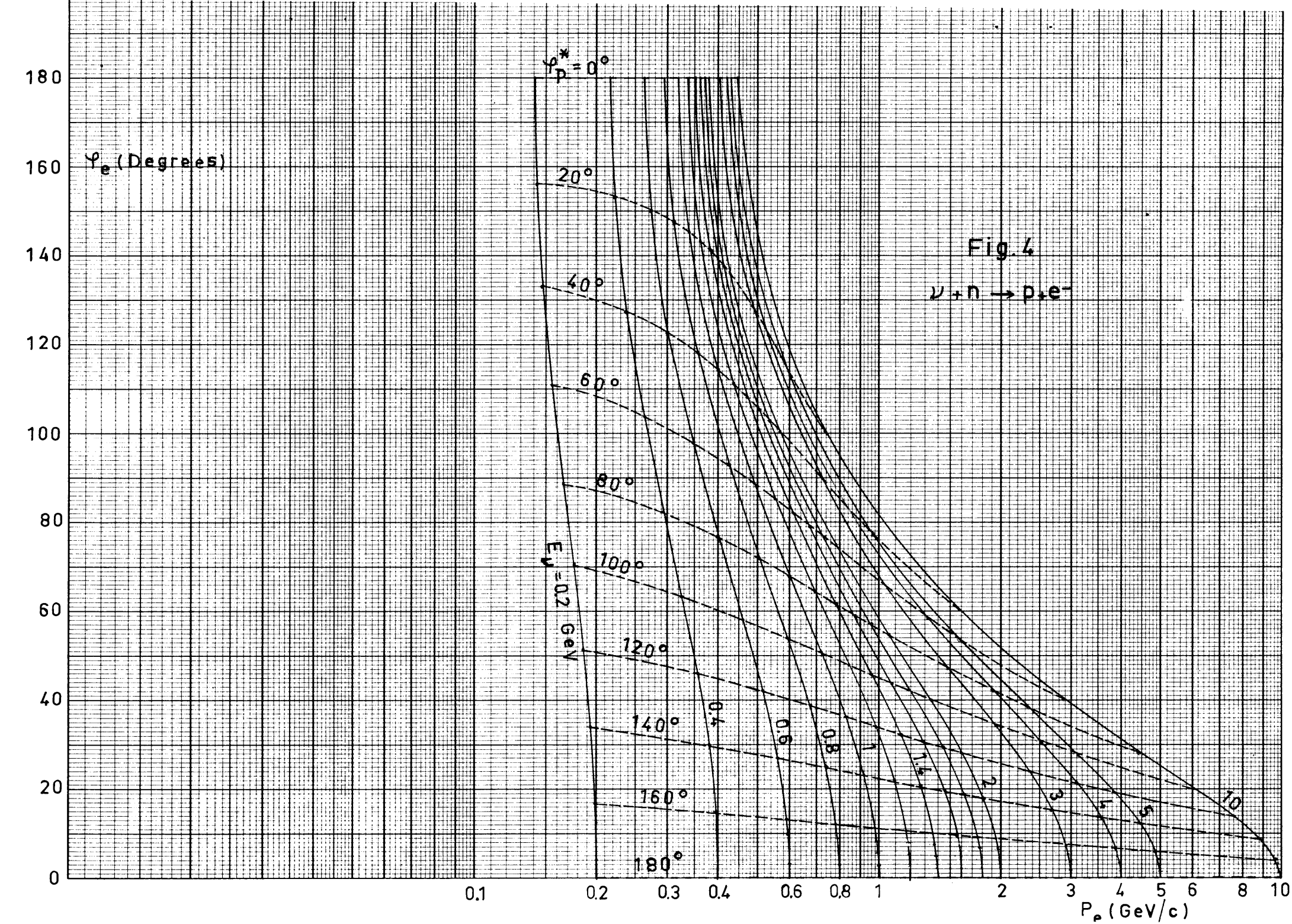

Fig. 4

$\nu + n \rightarrow p + e^-$

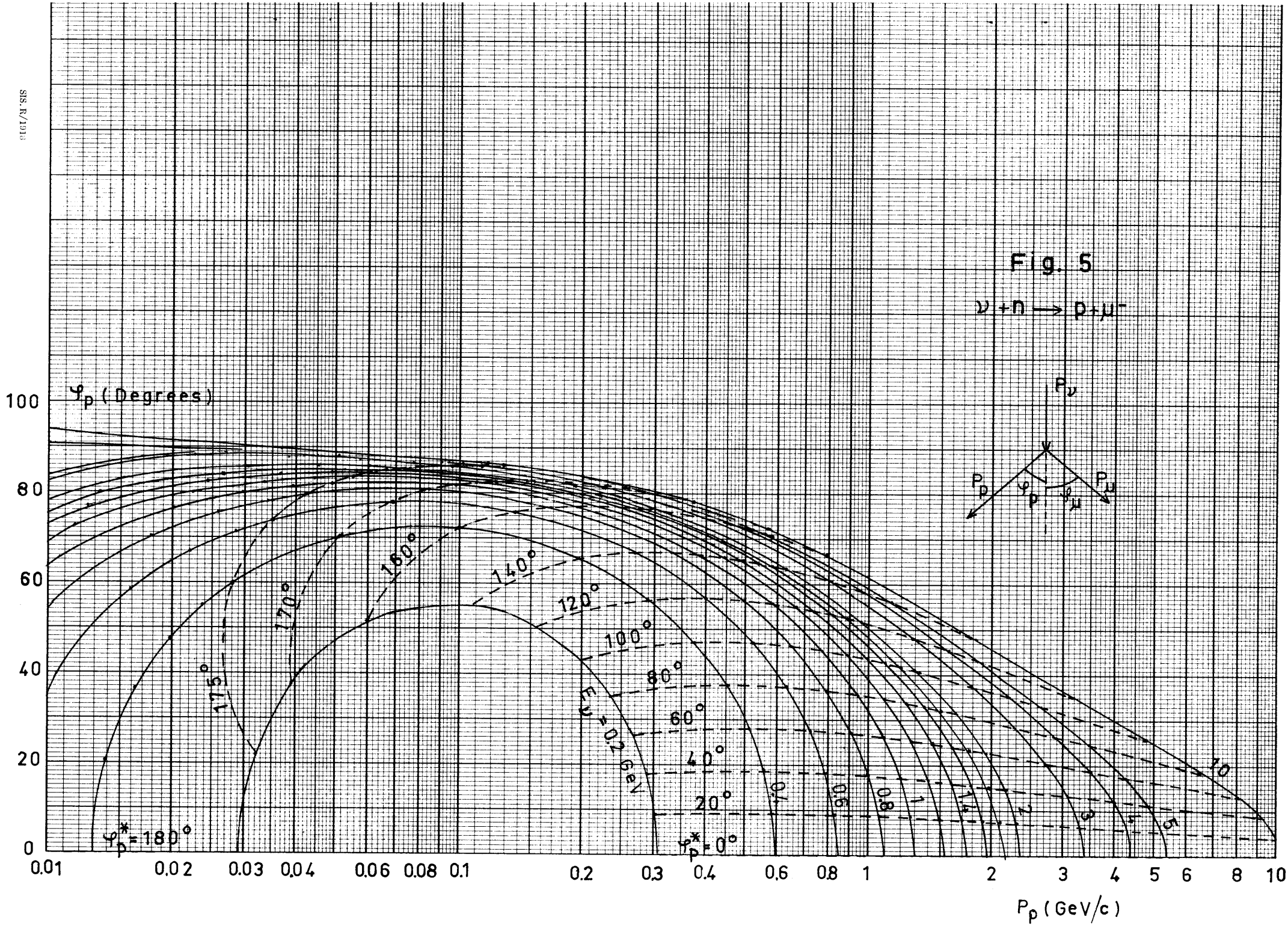
Fig. 5
ν + n → p + μ⁻
φp (Degrees)
Pν
Pp
φp
φμ
Pμ
100
80
60
40
20
0
0.01
0.02
0.03
0.04
0.06
0.08
0.1
0.2
0.3
0.4
0.6
0.8
1
2
3
4
5
6
8
10
Pp (GeV/c)
φp* = 180°
φp* = 0°
175°
170°
160°
140°
120°
100°
80°
60°
40°
20°
Eν = 0.2 GeV
0.4
0.6
0.8
1
2
3
4
5
10

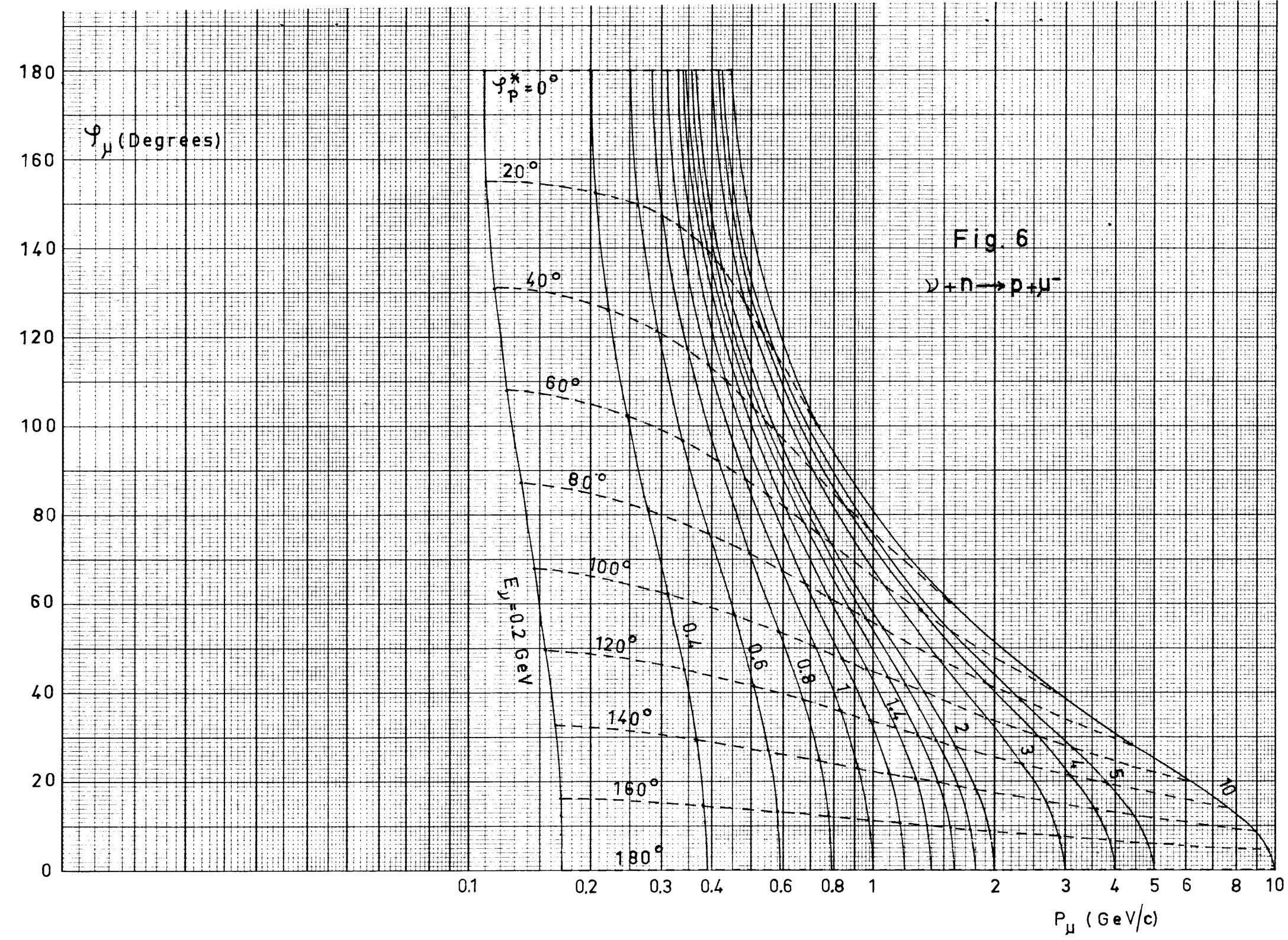
φ_μ (Degrees)
180
160
140
120
100
80
60
40
20
0
$\varphi_p^* = 0°$
20°
40°
60°
80°
100°
120°
140°
160°
180°
E_ν=0.2 GeV
0.4
0.6
0.8
1
1.4
2
3
4
5
10
0.1
0.2
0.3
0.4
0.6
0.8
1
2
3
4
5
6
8
10
P_μ (GeV/c)
Fig. 6
$\nu + n \rightarrow p + \mu^-$

TARGET 1

Target in pump manifold ($\varphi_0 = 0.032$ rad)
and on the equilibrium orbit ($Y_0 = 0$)

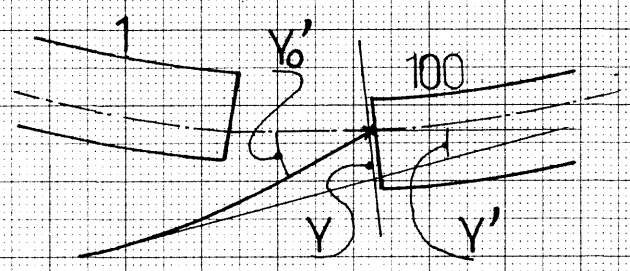

—— Refers to Y'

---- Refers to Y

See remark in Appendix 2 about the region of $Y_0' < 0$

Y (mm) Y'(m rad)

700 350 300 250 200 150 100 50 0

−.050 .050 .100 .150 .200

Y_0' (tan)

Fig. 7

SIS. R/1013

TARGET 2

Target in pump manifold ($Y_o = 0.032$ rad)
and on the equilibrium orbit ($Y_o = 0$)

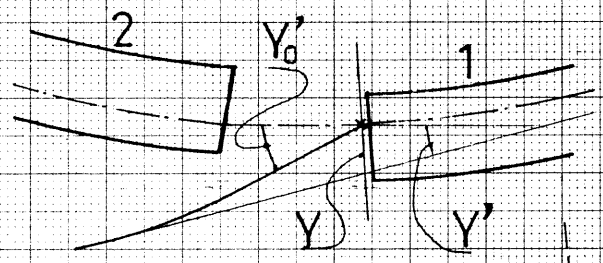

—Refers to Y'
----Refers to Y

Y (mm) Y'(m rad)

See remark in Appendix 2
about the region of $Y_o' < 0$

Y_o' (tan)

Fig. 8

TARGET 5

Target in pump manifold (φ_0=0.032rad)
and on the equilibrium orbit (Y_0=0)

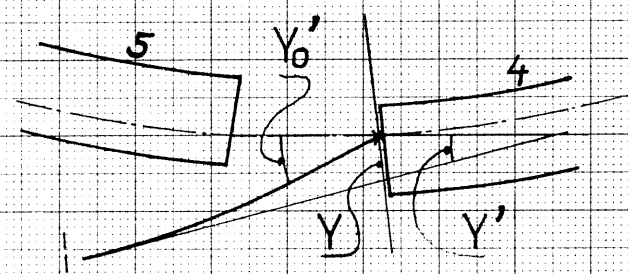

—Refers to Y'

----Refers to Y

See remark in
Appendix 2 about the
region of Y_0'<0

Y(mm) Y'(mrad)

Fig. 9

Y_0'(tan)

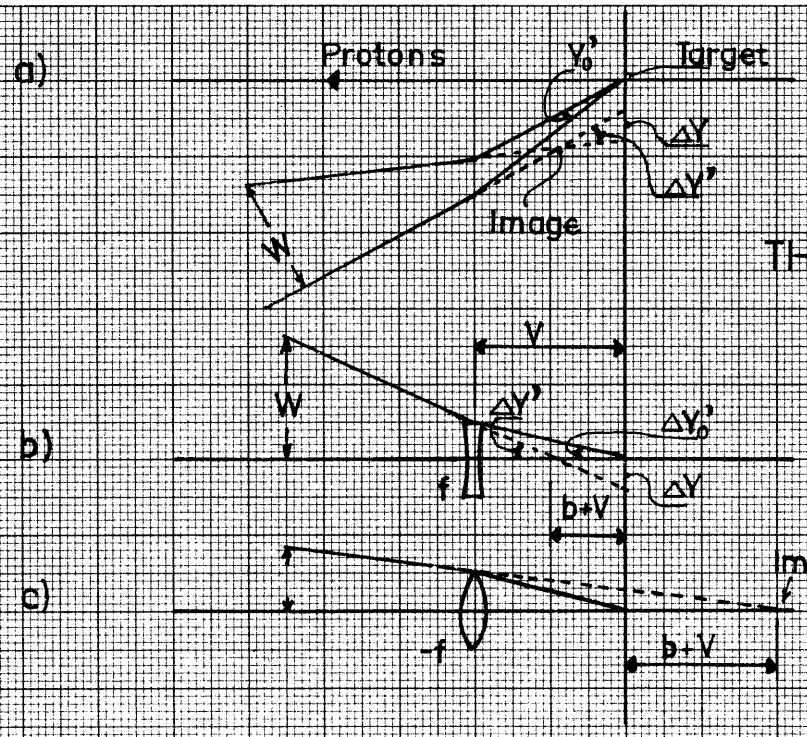

Fig.10

THIN LENS APPROXIMATION

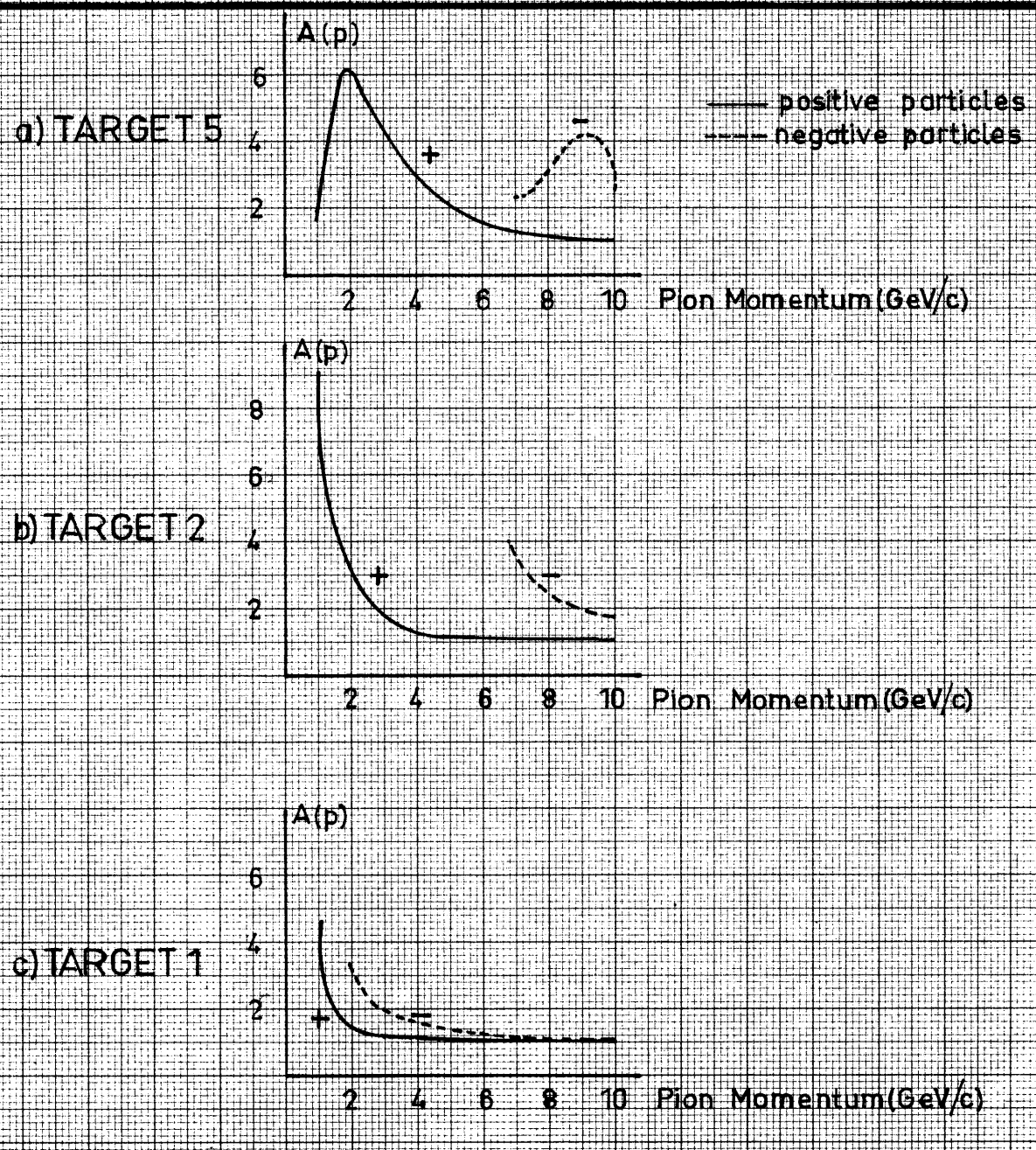

FOCUSING FACTOR A(p) AS A FUNTION OF MOMENTUM Fig.11